Journal of Mathematical Chemistry 4(1990)103–115

ON SUBSPECTRAL ACYCLIC MOLECULAR GRAPHS

Yuansheng JIANG* and Guangyao CHEN
Institute of Theoretical Chemistry, Jilin University, Changchun, People's Republic of China

Abstract

Based on the contraction and expansion of graphs, the subspectrality of acyclic molecular graphs is treated in a systematic way. The graphs containing eigenvalues $0, \pm 1$ and $\pm\sqrt{2}$ are discussed in detail, with emphasis on how to detect and construct the concealed species which can neither be recognized by symmetry considerations nor by the Heilbronner procedure. As a consequence, graphs and their counts have been given for species with numbers of vertices less than 16.

1. Introduction

The connectivity of a graph can be characterized by its adjacency matrix A in which rows and columns correspond to vertices. The elements are 1 when the row vertices and column vertices are connected by edges and 0 otherwise. The characteristic polynomial (CP) and eigenvalues play a fundamental role in interpreting properties in terms of structures. Tables of Hückel spectra and CPs are available elsewhere [1–3].

Considerable interest has developed for the recognition of the phenomenon of subspectrality evident in these tables; this has been reviewed in a monograph [4]. The most popular method used is symmetry analysis [5–8]. For instance, graphs 1 and 2 in fig. 1 have a symmetrical plane perpendicular to the molecular plane and passing

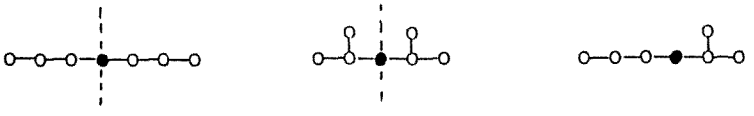

Fig. 1. Acyclic molecular graphs having common eigenvalues $0, \pm\sqrt{2}$. Dotted lines signify symmetry planes and solid circles represent nodes.

through the central vertex, splitting off an allyl fragment; thus, both of them have 0 and $\pm\sqrt{2}$ eigenvalues. However, coincidences between the eigenvalues of different molecular graphs occur much more frequently than can be explained by symmetry. As

*Also known as Yuan-sun Kiang.

one of the simple examples, graph 3 also contains eigenvalues 0 and $\pm\sqrt{2}$ without a symmetry plane.

In addition to symmetry considerations, the formula given by Heilbronner [9] is useful for the factorization of CPs [10–13]. The incident edges of nodes (solid circles in fig. 1) are suitable for erasing by splitting off the common factor $(x^3 - 2x)$; thus graphs 1–3 all have eigenvalues 0 and $\pm\sqrt{2}$. The third method, called embedding [14,15], is widely used to deal with benzenoid hydrocarbons.

If we examine Hosoya's table [3], which tabulates CPs of acyclic molecular graphs having $N \leq 10$ vertices, we can find dozens of subspectral species which can neither be interpreted by symmetry analysis nor by the Heilbronner formula. For example, there are four species with $N = 9$ sharing eigenvalues 0 and $\pm\sqrt{2}$, displayed in fig. 2. We will call them "concealed subspectral species" in our further discussion. We now ask the question: How are they recognized?

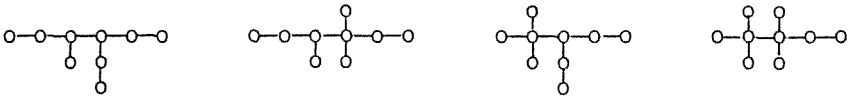

$x(x^2-1)(x^2-2)(x^4-5x^2-4)$ $x(x^2-2)(x^6-6x^4+5x^2-1)$ $x^3(x^2-2)(x^2-1)(x^2-4)$ $x^3(x^2-2)(x^4-6x^2+3)$

Fig. 2. Four concealed subspectral species having eigenvalues 0 and $\pm\sqrt{2}$, together with CPs given below each diagram [3].

In this paper, we develop a method to deal with the problem of subspectrality in general and present the result of acyclic molecular graphs in relation to eigenvalues $\pm\sqrt{2}$, ± 1 and 0 with emphasis on the concealed species.

2. Mathematical background

The characteristic polynomial of a graph G is defined as follows

$$P_G(x) = \det |xI - A|, \tag{1}$$

where I is the identity matrix and x is a variable. In correspondence, the weighted graph can be introduced, in which each vertex is subject to the value x instead of 0 but the edge keeps the standard weight 1. In the discussion of subspectrality, one substitutes x with special values $\pm\sqrt{2}$, ± 1, 0 and others. To avoid loops in the weighted graph, we put x or its substituted numerals as the standard weight for each vertex and assign to those vertices and edges numerals or symbols having weights different from standard values x and 1, respectively. We adopt this convention in later discussions.

The following theorem is fundamentally important for the detection and construction of concealed subspectral species.

THEOREM 1

Let G be the acyclic molecular graph with standard weight x and 1 for each of its vertices and edges, respectively. If G is partitioned into two subgraphs A and B by erasing one or more edges, then the CPs of G, B and A' satisfy

$$P_G(x) = P_B(x)P_{A'}(x), \quad \text{with } P_B(x) \neq 0, \tag{2}$$

where A' represents a modified version of A obtained by adjusting the weight of vertices and edges in A that are originally connected to B, namely,

(1) If vertex i in A is the common end of a set of erased edges ij_t ($t = 1, 2, \ldots, n$), which also means B is a multicomponent with vertices $j_1, j_2, \ldots, j_n$ in components $B_1, B_2, \ldots, B_n$, respectively, then the modification is limited to the vertex i with its weight y_i being

$$y_i = x - \sum_{t=1}^{n} P_{B_t - j_t}(x)/P_{B_t}(x), \tag{3}$$

where $B_t - j_t$ signifies the fragment obtained from B_t by deleting vertex j_t.

(2) If two (or more) ends of erased edges are left in A, then in addition to their modification according to eq. (3), an edge is generated between these two ends with weight equal to

$$b_{ik} = P_{B - \overline{jl}}(x)/P_B(x), \tag{4}$$

where ij and kl are erased edges with vertices i, k in A and j, l in B, $\overline{jl}$ represents the path starting from j to l and $B - \overline{jl}$ denotes the remaining fragment after removing this path from B.

The above statement is a simplified formulation of the original theorem appearing in refs. [16]. We emphasize its meaning by illustrating a simple example, the butadiene graph. This can be partitioned into A and B by erasing one or two edges, as shown in fig. 3. In scheme (1), the modified graph A'_1 comes from an ethene fragment,

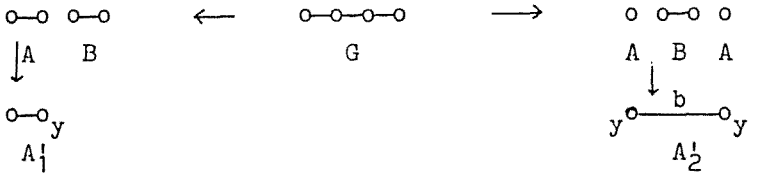

Scheme (1) Scheme (2)

Fig. 3.Partition of butadiene graph: the middle edge is erased in scheme (1) and two terminal edges are erased in scheme (2).

whereas in scheme (2), A'_2 is from a couple of vertices. The weight represented by symbols y and b displayed in A'_1 and A'_2 should be calculated according to eqs. (3) and (4). The results are

$$y = x - x/(x^2 - 1), \quad b = 1/(x^2 - 1). \tag{5}$$

Because fragments B, A'_1 and A'_2 are all ethene-like, we easily have the same CP for both schemes, i.e.

$$P_G(x) = P_B(x)P_{A'_1}(x) = (x^2 - 1)\,(xy - 1) = x^4 - 3x^2 + 1, \tag{6a}$$

$$P_G(x) = P_B(x)P_{A'_2}(x) = (x^2 - 1)(y^2 - b^2) = x^4 - 3x^2 + 1. \tag{6b}$$

The importance of eq. (3) for predicting whether a molecular graph G involves the eigenvalue x or not is quite obvious. This can be carried out by selecting a subgraph B or a set of components $B_1, B_2, \ldots, B_n$ according to theorem 1 such that the modified graph A' is simple enough to be tested on whether x is an eigenvalue, i.e.

$$P_{A'}(x) = 0, \tag{7}$$

or not. On the other hand, a fragment A' is able to couple with a set of fragments in the way fulfilling eq. (3), generating a large species G. If eq. (7) is satisfied, then x is the common eigenvalue of both species. In other words, the forward direction of eq. (3) means the contraction of a larger graph and the opposite corresponds to the expansion of a smaller one; both of them keep the essence of subspectrality invariant.

The situation seems of more significance when A' coincides with A, namely, $A' = A$. In this case, G shares eigenvalue x with its fragment A. We discuss the condition $A' = A$.

COROLLARY 1

If vertex i in A is connected to vertex j in B before erasing edge ij, then the condition that $A = A'$ is

$$P_{B-j}(x) = 0. \tag{8}$$

This is obvious on referring to eq. (3) and fig. 4.

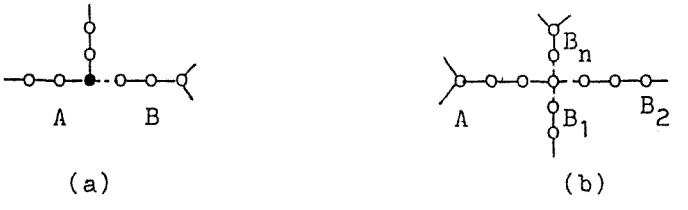

Fig. 4. (a) One edge (dotted line) is erased and vertex i (heavy circle) is a node of G; (b) n edges incident from vertex i in A are erased.

COROLLARY 2

If vertex i in A is connected to vertices j_1 in B_1, j_2 in B_2, . . . , j_n in B_n simultaneously before erasing (see fig. 4(b)), then the condition that $A' = A$ is

$$\sum_{t=1}^{n} P_{B_t - j_t}(x)/P_{B_t}(x) = 0. \tag{9}$$

This is also obvious on referring to eq. (3).

Corollary 1 is a different version of the Heilbronner formula when there exists a node in the considered graph G. It gives nothing new in relation to subspectrality. However, corollary 2 is essential to enquire into the details of topology inherent in the concealed acyclic subspectral species. The question is, how to carry out the detection and construction in general? For this purpose, corollary 3 is presented in addition.

COROLLARY 3

Suppose A is a monocomponent and eq. (9) is satisfied for every vertex in A when one erases all edges that A connects with other fragments in G. Then G shares eigenvalue x with its fragment A.

This is a generalization that eq. (9) holds for all vertices instead of a single one; therefore, $A' = A$ also holds.

In the remainder, we limit our discussion to concealed species with eigenvalues $\pm\sqrt{2}$, ± 1 or 0.

3. Subspectral species sharing $\pm\sqrt{2}$ eigenvalues

All acyclic molecular graphs are bipartite, satisfying the pairing theorem. Thus, only plus eigenvalues need be considered. The CP of a linear polyene involving n vertices has the following formula:

$$g_n(x) = \sum_{r=0}^{[n/2]} (-1)^r (n-r)!/(n-2r)! x^{n-2r}, \tag{10}$$

and we have its numerical value at $x = \sqrt{2}$ as follows:

$$g_n(\sqrt{2}) = (-1)^m(\delta_{n,4m} + \sqrt{2}\,\delta_{n,4m+1} + \delta_{n,4m+2}), \tag{11}$$

where $\delta_{a,b}$ represents the Kronecker symbol. With formula (11), the numerical values of the CP at $x = \sqrt{2}$ for acyclic species can be evaluated one by one. Graphs and symbols, together with the CP values at $x = \sqrt{2}$ for 22 elementary species with $N \leq 7$ vertices are displayed in fig. 5.

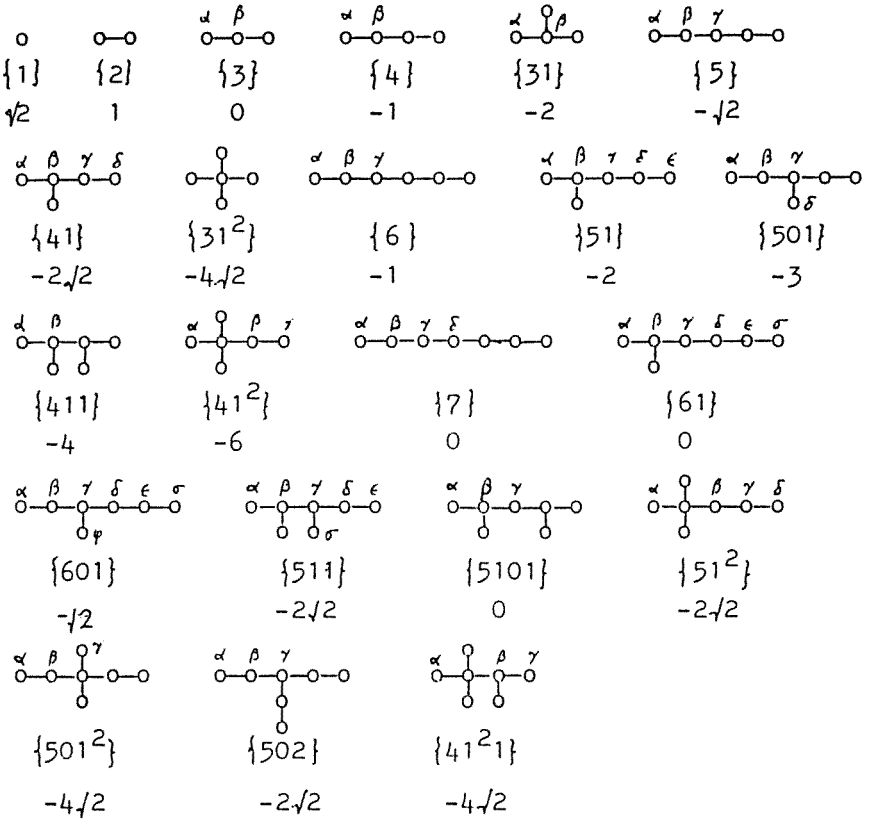

Fig. 5. Acyclic graphs ($N \leq 7$) with symbols and CP values cited below each diagram.

In fig. 5, the symbols $\alpha, \beta, \gamma, \ldots$ have been used to assign inequivalent vertices in each fragment, because inequivalent vertices of fragment B connected with a fixed vertex of A produce different graphs G. This has been implied in eq. (3), where y_i depends on the fragments $B_t - j_t$ ($t = 1, 2, \ldots$), in which vertex j_t in B_t is connected to vertex i in A before edge ij_t is erased. In other words, we should classify fragment B into subspecies $\{B\}^{\alpha}$, $\{B\}^{\beta}, \ldots$, in accordance with which vertex is connected.

Next, we can tabulate numerical values of $-P_{B-j}(\sqrt{2})/P_B(\sqrt{2})$ for individuals cited in fig. 5, provided $P_B(\sqrt{2}) \neq 0$. Sometimes, several $\{B\}^{j}$'s give an equal increment. For example, the following three contractions result in a common value $-1/\sqrt{2}$:

$$\begin{aligned} \{1\} \quad &: \; -1/P_{\{1\}}(\sqrt{2}) = -1/\sqrt{2}, \\ \{5\}^{\alpha} \quad &: \; -P_{\{4\}}(\sqrt{2})/P_{\{5\}}(\sqrt{2}) = -1/\sqrt{2}, \\ \{41\}^{\delta} \quad &: \; -P_{\{31\}}(\sqrt{2})/P_{\{41\}}(\sqrt{2}) = -1/\sqrt{2}. \end{aligned} \tag{12}$$

This results from the fact that vertices α in $\{5\}$ and δ in $\{41\}$ are nodes; thus, contractions with respect to $\{5\}^{\alpha}$ and $\{41\}^{\delta}$ are deducible from that of $\{1\}$. This means

that among the three modes of contraction discussed above, only that of $B = \{1\}$ is fundamental. We tabulate the increments of vertex weight for fundamental contractions in table 1.

Table 1

Numerical values of $-P_{B-j}(\sqrt{2})/P_B(\sqrt{2})$ for fundamental contractions with $N \leq 7$

$\{1\}$	$\{5\}^{\gamma}$	$\{41\}^{\beta}$	$\{2\}$	$\{4\}^{\beta}$	$\{31\}^{\beta}$	
$-\sqrt{2}/2$	$\sqrt{2}/2$	$\sqrt{2}/2$	$-\sqrt{2}$	$\sqrt{2}$	$\sqrt{2}$	
$\{41\}^{\alpha}$	$\{31^2\}^{\alpha}$	$\{502\}^{\gamma}$	$\{511\}^{\alpha}$	$\{501^2\}^{\alpha}$	$\{502\}^{\alpha}$	$\{41^21\}^{\alpha}$
$-\sqrt{2}/4$	$-\sqrt{2}/4$	$\sqrt{2}/4$	$-3\sqrt{2}/4$	$-3\sqrt{2}/4$	$-3\sqrt{2}/4$	$-3\sqrt{2}/4$
$\{41^2\}^{\beta}$	$\{41^2\}^{\gamma}$	$\{501\}^{\beta}$	$\{501\}^{\delta}$	$\{501\}^{\gamma}$	$\{501\}^{\alpha}$	$\{41^2\}^{\alpha}$
$-\sqrt{2}/3$	$-\sqrt{2}/3$	$-\sqrt{2}/3$	$-\sqrt{2}/3$	$\sqrt{2}/3$	$-2\sqrt{2}/3$	$-2\sqrt{2}/3$
$\{4\}^{\alpha}$	$\{31\}^{\alpha}$	$\{5\}^{\beta}$	$\{41\}^{\gamma}$			
0	0	0	0			

Based on table 1, the acyclic graphs sharing eigenvalues $\pm\sqrt{2}$ are easily constructed according to theorem 1 or corollaries 2 and 3. Let us start from the smallest graph $\{1\}$ with $x = 0$, namely, we put $A' = \{1\}$ with a zero weight for its vertex. Obviously, we have

$$P_{\{1\}}(0) = 0. \tag{13}$$

Because 0 can be taken as $\sqrt{2} - \sqrt{2}$, where $\sqrt{2}$ is equal to the standard vertex weight and $-\sqrt{2}$ corresponds to the increment for the contraction of $\{2\}$ displayed in the first row of table 1, in accordance with theorem 1 we have

$$P_{\{2\}}(\sqrt{2})P_{\{1\}}(0) = P_{\{3\}}(\sqrt{2}) = 0, \tag{14}$$

and we arrive at that allyl graph $\{3\}$ involving eigenvalues $\pm\sqrt{2}$. Similarly, one can write $0 = \sqrt{2} - \sqrt{2}/2 - \sqrt{2}/4 - \sqrt{2}/4$, where $-\sqrt{2}/2$ is equal to the increment that $\{1\}$ is being contracted and $-\sqrt{2}/4$ comes from either one of the contractions of $\{41\}^{\alpha}$ and $\{31^2\}^{\alpha}$. Therefore, three concealed subspectral species with $N = 12$ sharing eigenvalues $\pm\sqrt{2}$ are generated (see fig. 6). Furthermore, 0 can be equal to the algebraic sum

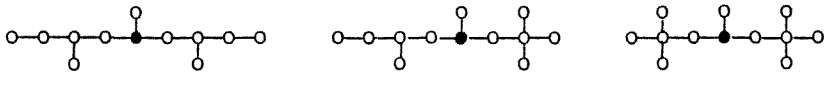

Fig. 6. Concealed subspectral species with $N = 12$; the solid vertex signifies A', the fragment starting the expansion.

$\sqrt{2} - 3\sqrt{2}/4 - \sqrt{2}/4$, where $-3\sqrt{2}/4$ is the common increment of contractions with respect to fragments $\{511\}^{\alpha}$, $\{501^2\}^{\alpha}$, $\{502\}^{\alpha}$ and $\{41^21\}^{\alpha}$. Therefore, eight concealed species with $N = 13$ can be constructed (see fig. 7).

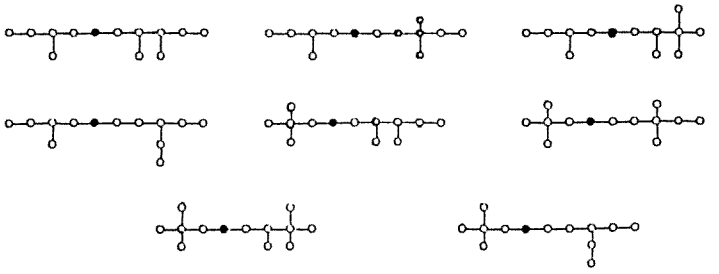

Fig. 7. Eight concealed subspectral species ($N = 13$) sharing eigenvalues $\pm\sqrt{2}$.

The second channel for the construction of concealed species sharing eigenvalues $\pm\sqrt{2}$ can be initiated by putting $A' = A = \{3\}$. According to corollary 2 or 3, a set of fragments with zero sum of increments of contraction (satisfying eq. (9)) can connect to either one or two vertices of the allyl graph without loss of $\pm\sqrt{2}$ eigenvalues. On consulting table 1, these zero sums can at first be supposed to be $-\sqrt{2}/2 + \sqrt{2}/2$, $-\sqrt{2} + \sqrt{2}$ and $-\sqrt{2}/2 - \sqrt{2}/2 + \sqrt{2}$. They correspond to the six modes of contraction shown below:

$$
\begin{aligned}
0 = -\sqrt{2}/2 + \sqrt{2}/2: &\qquad B_1 = \{1\},\ B_2 = \{5\}^{\gamma} \text{ or } \{41\}^{\beta};\\
0 = -\sqrt{2} + \sqrt{2}: &\qquad B_1 = \{2\},\ B_2 = \{4\}^{\beta} \text{ or } \{31\}^{\beta};\\
0 = -\sqrt{2}/2 - \sqrt{2}/2 + \sqrt{2}: &\qquad B_1 = \{1\},\ B_2 = \{1\},\ B_3 = \{4\}^{\beta} \text{ or } \{31\}^{\beta};
\end{aligned}
\tag{15}
$$

and generate 12 species with $N = 9$ vertices sharing eigenvalues $\pm\sqrt{2}$ in total if one vertex in the allyl graph is used for expansion. However, only four of them are distinguishable, which have been displayed in fig. 2.

Furthermore, if two vertices in the allyl graph are subject to expansion in accordance with eq. (15) simultaneously, then concealed species of 15 vertices are produced. In the case that both are terminal vertices, $6 \times 7/2 = 21$ species result because of symmetry. On the other hand, if one of them is the central vertex, $6 \times 6 = 36$ species can be, in principle, produced. However, due to the limitation that each vertex has degree no more than 4 in acyclic molecular graphs, only 24 species are allowed in practice. These two sets of acyclic species sharing eigenvalues $\pm\sqrt{2}$ with $N = 15$ are displayed in fig. 8, where $\{3\}$, playing the role of fragment A ($A = A'$) for the expansion, has been marked with solid vertices for clarity.

Still, there are 12 species with $N = 15$ which can be constructed by attaching either one set of fragments at the end of the allyl graph, followed by the connection of

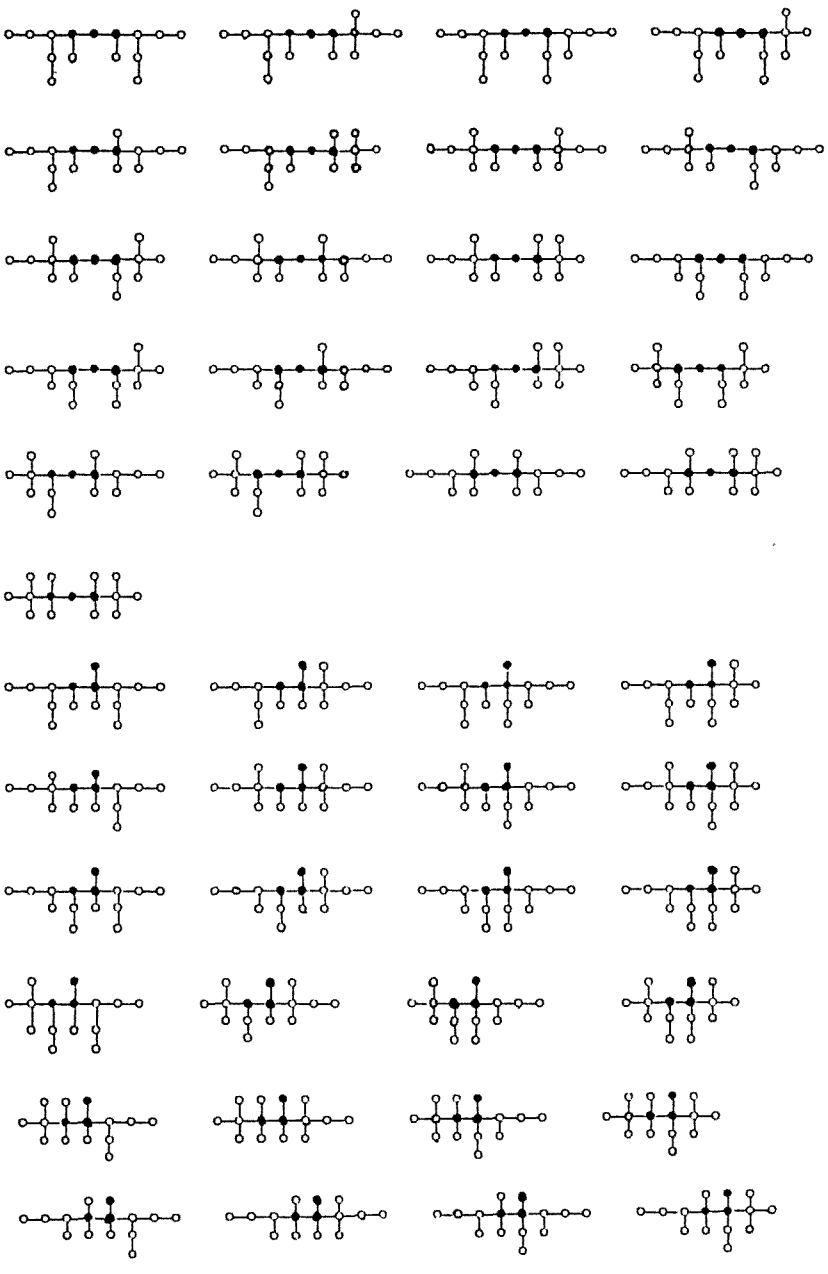

Fig. 8. Forty-five concealed subspectral species (N = 15) sharing eigenvalues $\pm\sqrt{2}$ formed from {3} by utilizing two vertices.

another set of fragments shown in eq. (15). These are displayed in fig. 9, where we use stars to show vertices at which the second expansions take place.

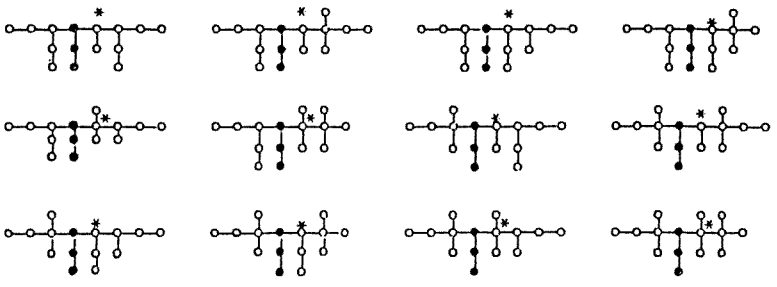

Fig. 9. Twelve concealed subspectral species (N = 15) sharing eigenvalues $\pm\sqrt{2}$ produced from {3} by successive expansions.

One of the additional zero sums is $0 = -\sqrt{2}/3 + \sqrt{2}/3$, where $-\sqrt{2}/3$ represents the increment of contraction of either one of the four fragments $\{501\}^{\beta}$, $\{501\}^{\delta}$, $\{41^2\}^{\beta}$ and $\{41^2\}^{\gamma}$, while $\sqrt{2}/3$ corresponds to $\{501\}^{\gamma}$. Both kinds of fragments can connect to the end or central vertex of {3}, producing eight species sharing $\pm\sqrt{2}$ with N = 15 vertices, as shown in fig. 10. Another zero sum, $0 = -\sqrt{2}/4 + \sqrt{2}/4$, induces the four concealed species displayed in fig. 11.

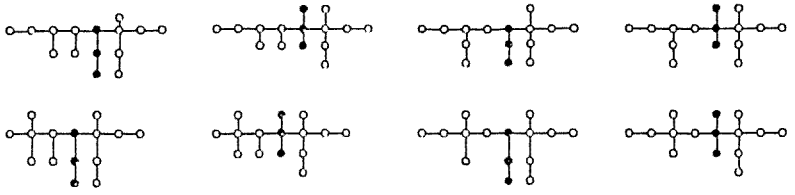

Fig. 10. Eight concealed subspectral species (N = 15) sharing eigenvalues $\pm\sqrt{2}$ derived in accordance with the zero sum $0 = -\sqrt{2}/3 + \sqrt{2}/3$.

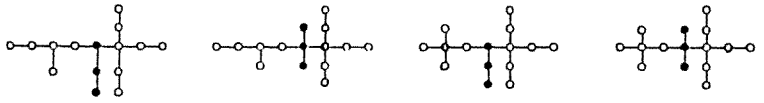

Fig. 11. Four species (N = 15) sharing eigenvalues $\pm\sqrt{2}$ derived with respect to the zero sum $0 = -\sqrt{2}/4 + \sqrt{2}/4$.

Thus, we have 69 concealed subspectral species with N = 15 that involve eigenvalues $\pm\sqrt{2}$. We tabulate the counts of such species with $N \leq 15$ vertices in table 2.

Table 2

Counts of concealed acyclic subspectral species sharing eigenvalues $\pm\sqrt{2}$ ($N \leq 15$)

N	1	2	3	4	5	6	7	8	9	10	11	12	13	14	15
Count	0	0	1	0	0	0	0	0	4	0	0	3	8	0	69

4. Subspectrality with eigenvalues ±1

Analogously, we can easily perform and find the increments of contractions $-P_{B-j}(1)/P_B(1)$ which are fundamental for the fragments displayed in fig. 5. They are listed in table 3.

Table 3

Numerical values of $-P_{B-j}(1)/P_B(1)$ for fundamental contractions with $N \leq 7$

$\{1\}$	$\{41\}^{\gamma}$	$\{3\}^{\beta}$	$\{51\}^{\varepsilon}$	$\{41^21\}^{\gamma}$	$\{31\}^{\alpha}$	$\{61\}^{\sigma}$	$\{31\}^{\beta}$	$\{61\}^{\epsilon}$	$\{51^2\}^{\delta}$
−1	−1	1	1	1	−1/2	−1/2	1/2	1/2	1/2
$\{51^2\}^{\gamma}$	$\{41\}^{\delta}$	$\{41^2\}^{\beta}$	$\{51\}^{\delta}$	$\{41^21\}^{\beta}$	$\{31^2\}$	$\{5101\}^{\beta}$	$\{5101\}^{\alpha}$	$\{5101\}^{\gamma}$	$\{41^2\}^{\alpha}$
3/2	−2	−2	2	2	−2/3	2/3	−1/3	−1/3	−3

Based on table 3, we can find all the concealed subspectral acyclic species sharing eigenvalues ±1 with $N \leq 15$. Their graphs are displayed in fig. 12, and counts are listed in table 4.

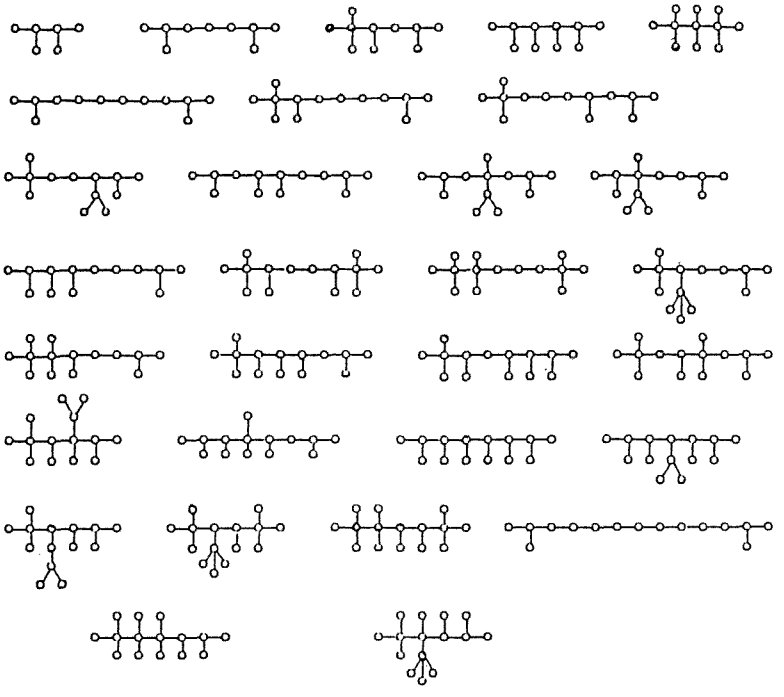

Fig. 12. Concealed subspectral acyclic species sharing eigenvalues ±1 with $N \leq 15$.

Table 4

Counts of concealed acyclic subspectral species sharing eigenvalues ±1 with $N \leq 15$

N	1	2	3	4	5	6	7	8	9	10	11	12	13	14	15
Count	0	1	0	0	0	1	0	0	1	2	1	1	7	12	5

5. Eigenvalue 0

The present approach has been used to deal with concealed non-Kekuléans, benzenoid hydrocarbons with 0 eigenvalue which cannot be detected by the coloring process [17]. For acyclic molecular graphs, coloring of vertices would in general also fail to determine the existence of zero eigenvalues. For example, the diradicals in fig. 13 have, by inspection, an equal number of starred and unstarred vertices.

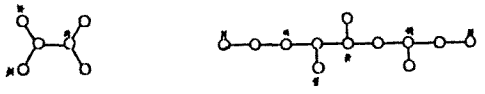

Fig. 13. Diradicals with equal bi-colored vertices.

This can be avoided by utilizing the following corollary.

COROLLARY 4

Zero eigenvalues can be determined by successively deleting terminal ethene fragments from the acyclic graph concerned until there remain isolated vertices solely. These isolated vertices enumerate zero eigenvalues therein.

In fig. 14, three simple examples are shown for illustration, where the deleted ethene fragments have been enveloped with ellipses for clarity and n_0 represents the number of zero eigenvalues.

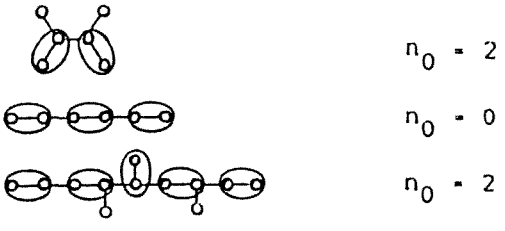

Fig. 14. Concealed acyclic species sharing 0 eigenvalue.

Acknowledgement

The authors gratefully acknowledge the support of the Chinese NSF.

References

[1] C. Coulson and A. Streitwieser, *Dictionary of π-Electron Calculations* (Freeman, San Francisco, 1965).
[2] E. Heilbronner and P.R. Straub, *HMO, Hückel Molecular Orbitals* (Springer-Verlag, Berlin, 1966).
[3] K. Mizutani, K. Kawasaki and H. Hosoya, Natural Science Report No. 22, Ochanomizu University (1971), p. 39.
[4] N. Trinajstić, *Chemical Graph Theory* (CRC, Boca Raton, FL, 1983).
[5] S.S. D'Amato, B.M. Gimarc and N. Trinajstić, Croat. Chim. Acta 54(1981)1.
[6] S.S. D'Amato, Mol. Phys. 37(1979)1363; Theor. Chim. Acta 53(1979)319.
[7] B.J. McClelland, J. Chem. Soc. Faraday Trans. II, 70(1974)1453; 78(1982)911.
[8] R.B. King, Theor. Chim. Acta 44(1977)223.
[9] E. Heilbronner, Helv. Chim. Acta 36(1953)170.
[10] T.Živković, N. Trinajstić and M. Randić, Croat. Chim. Acta 49(1977)89.
[11] W.T. Dixon, J. Chem. Soc. Faraday Trans. II, 72(1976)282.
[12] M. Randić, B. Baker and A.F. Kleiner, Int. J. Quant. Chem. S19(1985)107.
[13] E.C. Kirby, J. Math. Chem. 1(1987)175.
[14] G.G. Hall, Trans. Faraday Soc. 53(1957)573; Mol. Phys. 33(1977)551; Inst. Math. Appl. 17(1981)70.
[15] J.R. Dias, J. Mol. Struct. (Theochem.) 149(1987)213; 165(1988)125; J. Chem. Educ. 64(1987)213.
[16] Y.-S. Kiang, Int. J. Quant. Chem. S15(1981)293;
Y. Jiang, Scientia Sinica B25(1982)681; B27(1984)236.
[17] Y. Jiang and G.Y. Chen, *Studies in Physical and Theoretical Chemistry*, Vol. 63 (Elsevier, Amsteram, 1989), p. 107.